

# Analytic continuation average spectrum method for quantum liquids

David R. Reichman

*Department of Chemistry, Columbia University, 3000 Broadway, New York, New York 10027*

Eran Rabani

*School of Chemistry, The Sackler Faculty of Exact Sciences, Tel Aviv University, Tel Aviv 69978, Israel*

(Dated: November 1, 2018)

We revisit the problem of determining the real-frequency density response in quantum fluids via analytical continuation of imaginary-time quantum Monte Carlo data. We demonstrate that the average spectrum method (ASM) is capable of revealing resolved modes in the dynamic structure factor of both *ortho*-deuterium and liquid *para*-hydrogen, in agreement with experiments and quantum mode-coupling theories, while the maximum entropy approach yields only a smooth unimodal spectrum. Outstanding issues are discussed. Our work provides the first application of the ASM method in realistic off-lattice systems.

## I. INTRODUCTION

The computation of real-time correlation functions in condensed phase quantum systems is a challenging problem for which there is no universally applicable approach. This fact has necessitated the development of a variety of powerful methods ranging from exact numerical approaches to approximate theories.<sup>1,2,3,4,5,6,7,8,9,10,11,12,13,14,15,16,17</sup> The choice of method will in general depend on the type, dimensionality, and size of the system of interest as well as the external thermodynamic conditions under consideration.

The problems that plague exact real-time approaches are generally absent in imaginary time.<sup>18</sup> The dynamical sign problem, which renders most direct real time Monte Carlo simulations infeasible, is avoided in imaginary time. In principle, this means that a well defined Wick rotation may be used to recover real time information and excitation spectra.<sup>19</sup> If the precise analytical form of the correlation function is known in imaginary time, rotation in the complex time plane is straight forward. However in most cases of interest the imaginary time correlation function must be determined numerically via quantum Monte Carlo. In practice, analytic continuation in this case is numerically unstable and highly sensitive to statistical error.<sup>20</sup>

The most commonly used technique for the numerical analytical continuation of imaginary time quantum Monte Carlo data is the maximum entropy (MaxEnt) method.<sup>20,21,22,23,24,25,26,27,28,29,30,31,32,33,34,35</sup> In MaxEnt, the optimal fit of the data is defined in a Bayesian manner as the most likely fit that emerges from the competition between the  $\chi^2$  goodness-of-fit and an entropic prior  $S$ . MaxEnt generally requires an additional means to determine the prefactor  $\alpha$  (“temperature”) of the entropy term. Once determined, MaxEnt provides a statistically rigorous and unique fit for the spectral function. The strength of the MaxEnt method is that it generally provides good estimates of spectral area in the correct region of frequency space. However numerous studies have shown that, in general, MaxEnt solutions tend to

be too broad and smooth and often lack clearly defined peaks.<sup>36,37</sup> Other approaches have been devised to overcome this “smoothness” problem but these approaches have not met with much general success.

While MaxEnt provides a Bayesian estimate of the most likely fit, a different approach may be devised based on the notion of averaging over a sequence of possible solutions. Such approaches are called stochastic analytic continuation methods or average spectrum methods (ASM).<sup>38,39,40</sup> One justification for such a procedure is the fact that MaxEnt solutions for different values of  $\alpha$  may have spurious features that vanish or are diminished when averaged. This type of approach was independently suggested for the continuation of imaginary time quantum Monte Carlo data by White and Sandvik,<sup>38,41</sup> while similar ideas have been used in other fields.<sup>42,43</sup> While these methods have been put forward on rather heuristic grounds, the results generated in several studies give support to the notion that features not detected by MaxEnt may be faithfully revealed. Beach has provided a more secure theoretical foundation for such an approach by constructing a version of an ASM for which MaxEnt is the mean field limit.<sup>44</sup> Thus, one may view the ASM as including fluctuations not incorporated in the MaxEnt method.

In this work, we will use a variant of the ASM approach outlined by Slyjuasen<sup>40</sup> to calculate the dynamic structure factor of both liquid *ortho*-deuterium and liquid *para*-hydrogen. Such cases are useful because extensive experimental results exist in these systems that show features that are not captured by MaxEnt. While the ASM approach used here is more computationally demanding than MaxEnt, we find that this approach is capable of revealing such subtle features. Not surprisingly, the approach fares better for higher quality of the Monte Carlo data. Our work provides the first application of the ASM for analytical continuation of quantum Monte Carlo data for off-lattice systems with continuous potentials.

The outline of the paper is as follows: In Sec. II we outline the average spectrum method. Sec. III describes the model of liquid *ortho*-deuterium and liquid *para*-hydrogen, provides the technical Monte Carlo and in-

version details, and presents the results for the dynamics structure factor of both liquids. In Sec. IV we conclude.

## II. ANALYTIC CONTINUATION AVERAGE SPECTRUM METHOD

The analytic continuation of the intermediate scattering function<sup>24,33,34,37,45</sup> is based on the Fourier relation between the dynamic structure factor  $S(q, \omega)$  and the intermediate scattering function  $F(q, t)$ :

$$F(q, t) = \frac{1}{2\pi} \int_{-\infty}^{\infty} d\omega e^{-i\omega t} S(q, \omega). \quad (1)$$

By performing the replacement  $t \rightarrow -i\tau$ , and using the detailed balance relation  $S(q, -\omega) = e^{-\beta\omega} S(q, \omega)$  we obtain

$$\tilde{F}(q, \tau) = \frac{1}{2\pi} \int_0^{\infty} d\omega \left[ e^{-\omega\tau} + e^{(\tau-\beta)\omega} \right] S(q, \omega), \quad (2)$$

where  $t, \tau \geq 0$ , and

$$\tilde{F}(q, \tau) = \frac{1}{Z} \frac{1}{N} \text{Tr} \left( e^{-\beta, H} e^{\tau H} \hat{\rho}_{\mathbf{q}}^{\dagger} e^{-\tau H} \hat{\rho}_{\mathbf{q}} \right). \quad (3)$$

Here,  $Z$  is the partition function, the quantum collective density operator is given by  $\hat{\rho}_{\mathbf{q}} = \sum_{\alpha=1}^N e^{i\mathbf{q} \cdot \hat{\mathbf{r}}_{\alpha}}$ ,  $N$  is the number of particles,  $\mathbf{q}$  the wave number, and  $\hat{r}_{\alpha}$  is the position operator of particle  $\alpha$ .

The reason for introducing the imaginary time intermediate scattering function,  $\tilde{F}(q, \tau)$ , is that, unlike its real time counterpart, it is straightforward to obtain it using an appropriate path-integral Monte Carlo (PIMC) simulation technique.<sup>46,47</sup> However, in order to obtain the dynamic structure factor and the real time intermediate scattering function one has to invert the integral in Eq. (2). Due to the singular nature of the integration kernel the inversion of Eq. (2) is an ill-posed problem. As a consequence, a direct approach to the inversion would lead to an uncontrollable amplification of the statistical noise in the data for  $\tilde{F}(q, \tau)$ , resulting in an infinite number of solutions that satisfy Eq. (2).

In the present study we apply the recently developed averaged spectrum method,<sup>40</sup> related to earlier stochastic continuation approaches,<sup>38,39,44</sup> to invert the integral in Eq. (2) to get  $S(q, \omega)$ . Following the notation of other analytic continuation methods, we will refer to  $\tilde{F}(q, \tau)$

as the data (input data generated from the PIMC approach),  $K(\tau, \omega) = e^{-\omega\tau} + e^{(\tau-\beta)\omega}$  as the singular kernel, and  $S(q, \omega)$  as the solution. Furthermore, in what follows, we will assume that both the imaginary time axis and the frequency axis are discretized such that  $\tau = j_{\tau} \delta\tau$  ( $j_{\tau} = 1, \dots, N_{\tau}$ ) and  $\omega = j_{\omega} \delta\omega$  ( $j_{\omega} = 1, \dots, N_{\omega}$ ). Hence, Eq. (2) in its discrete form is given by:

$$\tilde{F}_{j_{\tau}}(q) = \sum_{j_{\omega}=1}^{N_{\omega}} \delta\omega K_{j_{\tau}, j_{\omega}} S_{j_{\omega}}(q), \quad (4)$$

where for future reference, the vectors  $\tilde{\mathbf{F}}(q)$  and  $\mathbf{S}(q)$  describe the data and the solution in discrete space, with values given by  $\tilde{F}_{j_{\tau}}(q)$  and  $S_{j_{\omega}}(q)$ , respectively.

The basic idea behind the ASM is to pick the final solution for  $\mathbf{S}(q)$  as the average spectral function obtained by averaging over a posterior distribution:

$$\bar{\mathbf{S}}(q) = \frac{\int d|\mathbf{S}(q)| \mathbf{S}(q) P(\mathbf{S}(q) | \tilde{\mathbf{F}}(q))}{\int d|\mathbf{S}(q)| P(\mathbf{S}(q) | \tilde{\mathbf{F}}(q))}, \quad (5)$$

where  $\mathbf{S}(q)$  is a solution to Eq. (4) for a given input  $\tilde{\mathbf{F}}(q)$ , and the posterior distribution can be expressed using Bayes theorem as:<sup>20,48</sup>

$$P(\mathbf{S}(q) | \tilde{\mathbf{F}}(q)) = P(\tilde{\mathbf{F}}(q) | \mathbf{S}(q)) P(\mathbf{S}(q)). \quad (6)$$

In the above,  $P(\mathbf{S}(q))$  is the prior probability distribution and  $P(\tilde{\mathbf{F}}(q) | \mathbf{S}(q))$  is the likelihood function. In the present study we assume a uniform prior for all positive spectral functions with a zero moment that obeys the sum rule  $\sum K_{0, j_{\omega}} S_{j_{\omega}}(q) \delta\omega = \tilde{F}_0(q)$ . Thus, we can write  $P(\mathbf{S}(q))$  as:<sup>40</sup>

$$P(\mathbf{S}(q)) \propto \delta \left( \sum_{j_{\omega}} K_{0, j_{\omega}} S_{j_{\omega}}(q) \delta\omega - F_0(q) \right) \prod_{j_{\omega}} \Theta(S_{j_{\omega}}(q)), \quad (7)$$

where  $\delta(x)$  is Dirac's delta function and  $\Theta(x)$  is the Heaviside step function. The choice of the prior distributions can be tricky. In order to avoid any undesired bias in the inversion procedure, we limit the present study to the case of a uniform prior that meets the necessary sum rule described above.

The likelihood function appearing in Eq. (6) describing the fluctuations of the imaginary time data is assumed to be of a Gaussian form:

$$P(\tilde{\mathbf{F}}(q) | \mathbf{S}(q)) \propto \exp \left\{ -\frac{1}{2} \text{Tr} \sum_{i=1}^n (\tilde{\mathbf{F}}^i(q) - \tilde{\mathbf{F}}(q)^{\mathbf{S}(q)})^T \Sigma(q)^{-1} (\tilde{\mathbf{F}}^i(q) - \tilde{\mathbf{F}}(q)^{\mathbf{S}(q)}) \right\}, \quad (8)$$

where we have partitioned the PIMC data into  $n$  bins

each contains  $m$  measurements, the vector  $\tilde{\mathbf{F}}^i(q)$  is the

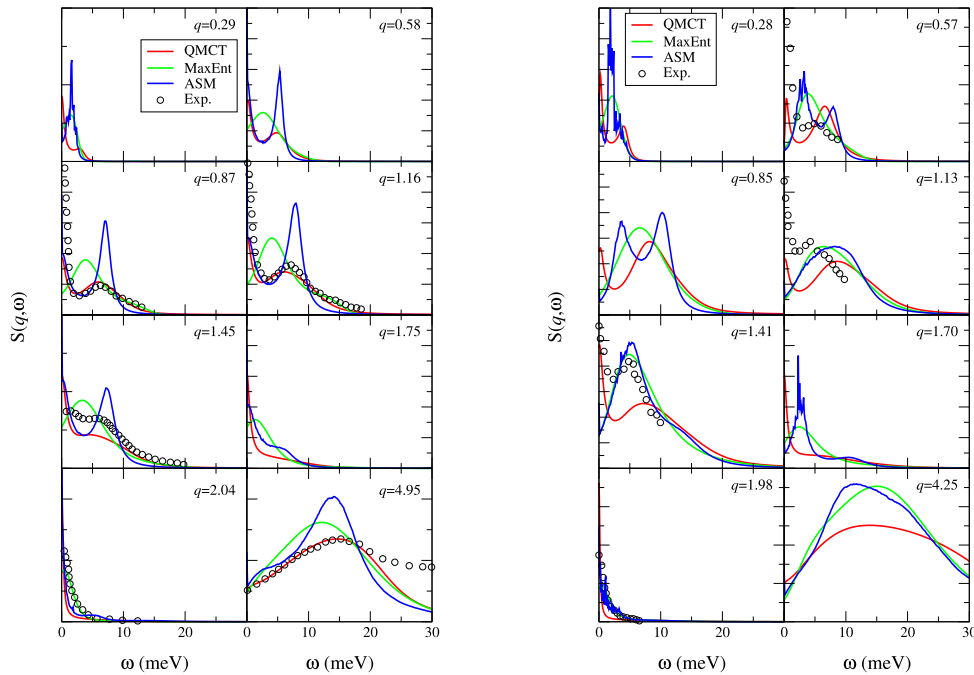


Figure 1: Plots of the dynamics structure factor for liquid *ortho*-deuterium (left panels) and liquid *para*-hydrogen (right panels) for different values of  $q$ . Experimental results are taken from Ref. 49 for liquid *ortho*-deuterium and from Ref. 50 for *para*-hydrogen. Values of  $q$  are in inverse .

average result for bin  $i$ , and  $\mathbf{F}(q)^{\mathbf{S}(q)}$  is the data vector corresponding to a specific solution  $\mathbf{S}(q)$ . The width of the Gaussian distribution is taken from the covariance matrix  $\Sigma(q)$  with elements of  $\Sigma(q)$  given by:

$$\Sigma_{j_\tau k_\tau}(q) = \frac{1}{n-1} \sum_i (\tilde{F}_{k_\tau}^i(q) - \tilde{F}_{k_\tau}(q)) (\tilde{F}_{j_\tau}^i(q) - \tilde{F}_{j_\tau}(q)). \quad (9)$$

The above expression for the likelihood function can further be simplified<sup>40</sup> to derive a working expression give by:

$$P(\tilde{\mathbf{F}}(q)|\mathbf{S}(q)) \propto \exp \left\{ -\frac{n}{2} E(\mathbf{S}(q)) \right\}, \quad (10)$$

with the “energy” function  $E(\mathbf{S}(q))$  given by:

$$E(\mathbf{S}(q)) = \text{Tr}(\tilde{\mathbf{F}}(q) - \tilde{\mathbf{F}}(q)^{\mathbf{S}(q)})^T \Sigma(q)^{-1} (\tilde{\mathbf{F}}(q) - \tilde{\mathbf{F}}(q)^{\mathbf{S}(q)}). \quad (11)$$

For readers who are interested in a more comprehensive discussion of the ASM we refer them to Refs. 38 and 40. Here, we have provided a short overview for completeness and note that the averaging procedure described above ensures that solutions  $(\mathbf{S}(q))$  which over-fit the noise in the data  $(\tilde{\mathbf{F}}(q))$  are averaged out, and thus the outcome is likely to be a smooth spectrum, with realistic features.

### III. MODEL AND RESULTS

The major goal of the present study is to conduct a direct comparison between the ASM, the

MaxEnt method, and the QMCT for collective density fluctuations in liquid *ortho*-deuterium and liquid *para*-hydrogen. Both liquids have been studied extensively over the past decade by many different techniques.<sup>11,30,33,34,37,45,51,52,53,54,55,56,57,58,59,60,61,62,63,64</sup> These and other studies show that they are characterized by quantum dynamical susceptibilities which are not reproducible using classical theories. Thus, these liquids are ideal to assess the accuracy of methods developed for quantum liquids and serve as canonical models in the field.

The static input required by the QMCT and the imaginary time intermediate scattering function required for the analytic continuation approaches were generated by PIMC simulations at  $T = 20.7\text{K}$  and  $\rho = 0.0254\text{\AA}^{-3}$  for liquid *ortho*-deuterium<sup>65</sup> and  $T = 14\text{K}$  and  $\rho = 0.0235\text{\AA}^{-3}$  for liquid *para*-hydrogen.<sup>66</sup> The PIMC simulations were done using the NVT ensemble with 256 particles interacting via the Silvera-Goldman potential,<sup>67,68</sup> where the entire molecule is described as a spherical particle, so the potential depends only on the radial distance between particles. The staging algorithm<sup>69</sup> for Monte Carlo chain moves was employed to compute the numerically exact input. The imaginary time interval was discretized into  $N_\tau$  Trotter slices of size  $\epsilon = \beta/N_\tau$  with  $N_\tau = 20$  and  $N_\tau = 50$  for liquid *ortho*-deuterium and liquid *para*-hydrogen, respectively. Approximately  $1-2 \times 10^6$  Monte Carlo passes were made, each pass consisted of attempting moves in all atoms and all the beads that were staged. Data collection was taken every 10

Monte Carlo steps, block averaging was done for  $m = 10$  and the total number of bins was set to  $n = 1 - 2 \times 10^4$ . The acceptance ratio was approximately 0.25 – 0.3 for both liquids.

In Fig. 1 we show the results for the dynamic structure factor  $S(q, \omega)$  for both liquids and for different values of  $q$ . The results are compared to the experiments of Mukherjee *et al.*<sup>49,70</sup> for *ortho*-deuterium and to the experiments of Bermejo *et al.*<sup>50,56</sup> for liquid *para*-hydrogen for selected values of  $q$  (the theoretical values of  $q$  are slightly different from the experiments due to the limitations associated with the constant volume simulation and finite size effects). Several important features are observed experimentally: First, the presence of a finite frequency peak that disappears around  $q = 1.4^{-1}$  signifying the presence of collective density fluctuations (this feature is not observed classically for these systems). Second, the presence of a low frequency peak associated with the long-time relaxation of density fluctuations. Finally, as  $q$  approaches  $q_{max}$  ( $q_{max} \approx 2^{-1}$  is the value of  $q$  where the static structure factor reaches its first maximum) one observes a quantum mechanical de Gennes narrowing of the dynamic structure factor.

These features are semi-quantitatively reproduced by the QMCT as shown in Fig. 1 (a full description of the method can be found in our previous publication<sup>37</sup>). In particular, the theory captures the position of both the low and high intensity peaks for liquid *ortho*-deuterium and slightly overestimates the position of the high frequency peak for liquid *para*-hydrogen. The width of the peaks, which are associated with the lifetime of density relaxation, are also captured by QMCT as is the quantum mechanical de Gennes narrowing of the dynamic structure factor. The overall good agreement between the QMCT and the experiments is remarkable and signifies the importance of the quantum mode-coupling portion to the memory kernel at long times.<sup>37,51,53,55</sup>

Turning to the MaxEnt results for  $S(q, \omega)$  (a full description of the calculation can be found elsewhere<sup>37</sup>), it becomes obvious that MaxEnt fails to provide a quan-

titative description of the density fluctuations in these liquids. It is well known that the MaxEnt approach often fails when several distinct spectral features appear that are closely spaced in frequency. This is clearly the case here where the MaxEnt approach predicts a single frequency peak instead of two, at a position that is approximately the averaged position of the two experimental peaks. Only when the dynamics are characterized by a single relaxation time, like the case at  $q_{max}$ , does the MaxEnt approach provides quantitative results.

The failure of the MaxEnt result poses a challenge for analytic continuation based methods. Can the inversion of Eq. (2) by other analytic continuation methods produce features that are not reproducible by MaxEnt? In order to address this problem, we need to average the spectrum over the posterior distribution, e.g. solve for the average spectrum as given by Eq. (5). The averaging procedure is best done by a Metropolis Monte Carlo approach described in Ref. 40. The basic idea behind the Monte Carlo procedure is to start with any guess for the spectrum  $\mathbf{S}(q)$  and then perform a Metropolis walk in the solution space to obtain different spectra  $\mathbf{S}(q)$  that are distributed according to posterior distribution  $P(\mathbf{S}(q)|\tilde{\mathbf{F}}(q))$ .

In practice, we follow the recipe of Ref. 40. First, we randomly choose a pair of neighboring frequencies,  $j_\omega$  and  $j_\omega + 1$ . We then select a random number  $\zeta = [-\alpha, \alpha]$  where  $\alpha = S_{j_\omega}(q)K_{0,j_\omega} + S_{j_\omega+1}(q)K_{0,j_\omega+1}$ , and make a trial move that preserve the sum rule  $\sum K_{0,j_\omega} S_{j_\omega}(q) \delta\omega = \tilde{F}_0(q)$ :

$$\begin{aligned} S_{j_\omega}^{new}(q) &= S_{j_\omega}(q) + \zeta \frac{K_{0,j_\omega+1}}{K_{0,j_\omega} + K_{0,j_\omega+1}} \\ S_{j_\omega+1}^{new}(q) &= S_{j_\omega+1}(q) - \zeta \frac{K_{0,j_\omega}}{K_{0,j_\omega} + K_{0,j_\omega+1}} \end{aligned} \quad (12)$$

The trial move is accepted only if  $S_{j_\omega+1}^{new}(q) \geq 0$  with the Metropolis probability given by:

$$P(\mathbf{S}(q) \rightarrow \mathbf{S}^{new}(q)) = P(\mathbf{S}^{new}(q)) \min \left\{ 1, \exp \left[ -\frac{n}{2} (E(\mathbf{S}^{new}(q)) - E(\mathbf{S}(q))) \right] \right\}, \quad (13)$$

where  $E(\mathbf{S}(q))$  is given by Eq. (11). In the present study we employ a simple Metropolis algorithm to sample the values of  $\mathbf{S}(q)$ . We did not encounter difficulties with sampling that require more sophisticated Monte Carlo procedures like parallel-tempering.<sup>40</sup> As a check, we started the Monte Carlo procedure from 10 different initial conditions. All the different runs converged to the same solution within the statistical noise of the Monte Carlo sampling. The ASM results shown in Fig. 1 where averaged over  $\approx 10^8$  Monte Carlo sweeps, each consist of

an attempt to change  $N_\omega = 512$  solution points.

The main and perhaps, unexpected, result is that the ASM captures qualitatively all feature observed experimentally for the dynamics structure factor, as shown in Fig. 1. Contrary to MaxEnt, the ASM reproduces the low and finite frequency peaks, albeit the fact that it somewhat underestimates the width of the finite frequency peak and also slightly overestimates the position of the low frequency peak. Overall, the ASM agrees better with the QMCT and with the experimental results

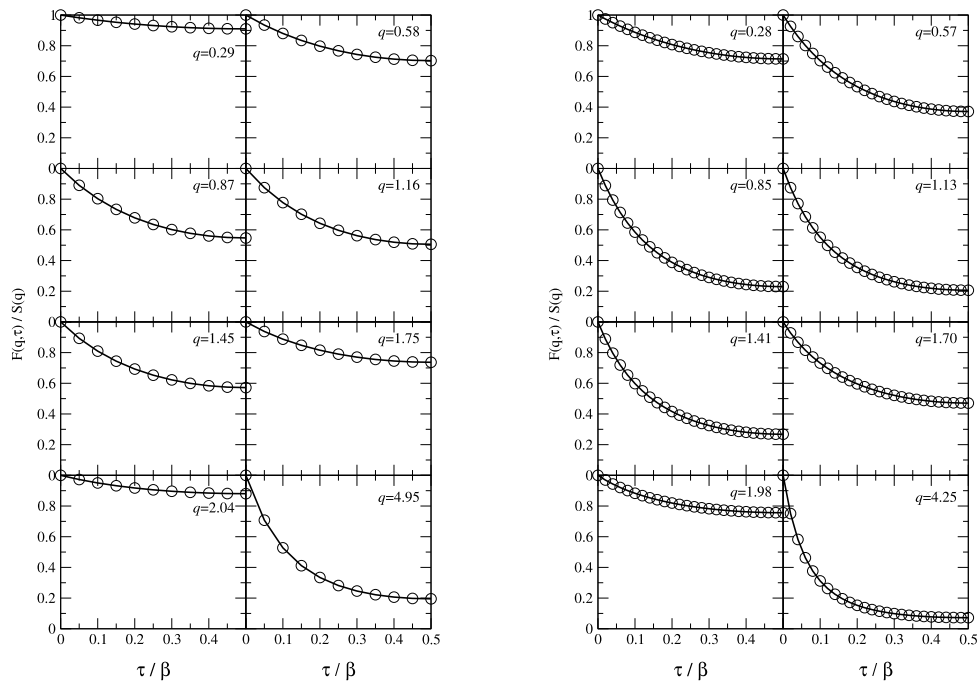


Figure 2: Plots of the imaginary time intermediate scattering function for liquid *ortho*-deuterium (left panels) and liquid *para*-hydrogen (right panels) for different values of  $q$ . Open circles represent the results obtained from the PIMC simulations and the solids lines are fits of the ASM to the PIMC results. Values of  $q$  are in inverse .

as compared to MaxEnt. The fact that there are features that are observed experimentally and captured by QMCT and ASM and not by MaxEnt method, indicate the superiority of the former approaches over MaxEnt.

Despite the semi-quantitative agreement of the QMCT and ASM approaches with experiments, there are still significant differences, as clearly is the case for liquid *para*-hydrogen. It still remains a challenge to determine the accuracy of both approaches since an exact solution for this many-body quantum mechanical problem is still (and may always be) out of reach. A direct comparison with experiments can be misleading, since several approximations are made for both QMCT and ASM. First, both are based on the assumption that the dynamics evolve over the potential energy taken from the work of Silvera and Goldman.<sup>67,68</sup> Furthermore, for simplicity, *para*-hydrogen and *ortho*-deuterium were treated as spherical particles, while experimentally this is not the case. Finally, for convenience, the simulations were done for the NVT ensemble while experiments are conducted at constant pressure (NPT ensemble). These approximation may lead to the difference observed between the theory and experiments, but the differences may also be attributed to the approximations made by QMCT and ASM for the dynamics itself. Nonetheless, the encouraging agreement between QMCT and ASM provides stronger support for their accuracy.

Before we conclude, in Fig. 2 we show the excellent agreement between the imaginary data generated by the PIMC simulations and imaginary data obtained by the

inversion of Eq. (2). As is well understood, only disagreement at this level can be used to draw decisive conclusion about the inversion process. However, it is quite satisfactory that the Monte Carlo procedure in the ASM leads to an excellent agreement for the imaginary time data.

#### IV. CONCLUSIONS

A comparison between the QMCT, MaxEnt method, and ASM has been made for the case of collective density fluctuations in liquid *ortho*-deuterium and liquid *para*-hydrogen. As far as we know, the present study is the first attempt to apply the ASM to dynamical susceptibilities for off-lattice models. We find that the main features observed experimentally for the cases discussed above are captured by QMCT and ASM, but not by MaxEnt. The results obtained by the ASM appear to coincide with the experimental results more closely in the case of *ortho*-deuterium. In this case the ASM produces results that are narrower than those seen in experiment. However, it should be expected that the theoretical spectrum is indeed sharper than that obtained in experiment because no instrumental broadening function is included in the theoretical calculations. The better agreement in the case of *ortho*-deuterium compared to *para*-hydrogen for the ASM may be a result of the better statistical quality of the data used in the *ortho*-deuterium case.

Our ASM results for the non-trivial examples presented here give strong motivation to continue the in-

vestigation of the ASM approach in other systems. One important problem worthy of reinvestigation is study of density fluctuations in superfluid helium. Boninsegni and Ceperley<sup>24</sup> studied this problem and found that the sharp features associated with roton peaks could not be reproduced by the MaxEnt approach. It would be interesting to see what the ASM yields for this challenging and important problem. Indeed, since the the ASM results presented here and by others provide clear evidence that analytic continuation based approaches are not limited to the case where dynamical susceptibilities are characterized by a single timescale, and since the ASM is a flexible approach suitable to the study of any type of correlation function for which imaginary time quantum Monte Carlo data can be generated, we expect that this approach will be further developed and utilized as a powerful means of extracting dynamical information from imaginary time simulations.

We would also like to add a word that at this stage it is still not entirely clear what should be trusted *a priori* in the ASM results and if the ASM is universally superior to MaxEnt. Unpublished work investigating the behav-

ior of both MaxEnt and the ASM in lattice models of the temperature and doping dependence near the Mott transition actually suggest that MaxEnt can in some cases provide a superior description of certain spectral features, but is inferior in its description of others.<sup>71</sup> For example MaxEnt fails completely in describing the Fermi liquid behavior of the self energy in the low frequency range while, rather surprisingly, the ASM does. Thus, we may conservatively suggest that at the very least, the ASM provides a complimentary and useful tool for extracting real time features from imaginary time quantum Monte Carlo data that appears to be superior to MaxEnt at least in its ability to uncover sharp spectral features. Assessing the accuracy of the ASM in a more systematic manner is another worthy direction of future research.

## V. ACKNOWLEDGEMENTS

DRR would like to thank the NSF for funding and Andy Millis for useful discussions.

- 
- <sup>1</sup> P. J. Rossky and J. D. Simon, *Nature* **370**, 263 (1994).  
<sup>2</sup> G. A. Voth, *Adv. Chem. Phys.* **XCIII**, 135 (1996).  
<sup>3</sup> N. Makri, *Ann. Rev. Phys. Chem.* **50**, 167 (1999).  
<sup>4</sup> S. A. Egorov, E. Rabani, and B. J. Berne, *J. Phys. Chem. B* **103**, 10978 (1999).  
<sup>5</sup> J. C. Tully, *Ann. Rev. Phys. Chem.* **51**, 153 (2000).  
<sup>6</sup> S. Hammes-Schiffer and S. R. Billeter, *Int. Rev. Phys. Chem.* **20**, 591 (2001).  
<sup>7</sup> G. Krilov, E. Sim, and B. J. Berne, *Chem. Phys.* **268**, 21 (2001).  
<sup>8</sup> W. H. Miller, *J. Phys. Chem. A* **105**, 2942 (2001).  
<sup>9</sup> I. R. Craig and D. E. Manolopoulos, *J. Chem. Phys.* **121**, 3368 (2004).  
<sup>10</sup> M. Thoss and H. B. Wang, *Ann. Rev. Phys. Chem.* **55**, 299 (2004).  
<sup>11</sup> E. Rabani and D. R. Reichman, *Ann. Rev. Phys. Chem.* **56**, 157 (2005).  
<sup>12</sup> R. Kapral, *Ann. Rev. Phys. Chem.* **57**, 129 (2006).  
<sup>13</sup> G. Hanna and R. Kapral, *Acc. Chem. Res.* **39**, 21 (2006).  
<sup>14</sup> W. R. Duncan and O. V. Prezhdo, *Ann. Rev. Phys. Chem.* **58**, 143 (2007).  
<sup>15</sup> R. Bulla, T. A. Costi, and D. Vollhardt, *Phys. Rev. B* **64**, 045103 (2001).  
<sup>16</sup> A. Georges, G. Kotliar, W. Krauth, and M. J. Rozenberg, *Rev. Mod. Phys.* **68**, 13 (1996).  
<sup>17</sup> S. R. White, *Phys. Rev. Lett.* **69**, 2863 (1992).  
<sup>18</sup> B. J. Berne and D. Thirumalai, *Annu. Rev. Phys. Chem.* **37**, 401 (1986).  
<sup>19</sup> G. Baym and N. D. Mermin, *J. Math. Phys.* **2**, 232 (1961).  
<sup>20</sup> M. Jarrell and J. E. Gubernatis, *Phys. Rep.* **269**, 134 (1996).  
<sup>21</sup> R. N. Silver, D. S. Sivia, and J. E. Gubernatis, *Phys. Rev. B* **41**, 2380 (1990).  
<sup>22</sup> J. E. Gubernatis, M. Jarrell, R. N. Silver, and D. S. Sivia, *Phys. Rev. B* **44**, 6011 (1991).  
<sup>23</sup> E. Gallicchio and B. J. Berne, *J. Chem. Phys.* **101**, 9909 (1994).  
<sup>24</sup> M. Boninsegni and D. M. Ceperley, *J. Low Temp. Phys.* **104**, 339 (1996).  
<sup>25</sup> E. Gallicchio and B. J. Berne, *J. Chem. Phys.* **105**, 7064 (1996).  
<sup>26</sup> G. Krilov and B. J. Berne, *J. Chem. Phys.* **111**, 9147 (1999).  
<sup>27</sup> E. Rabani, G. Krilov, and B. J. Berne, *J. Chem. Phys.* **112**, 2605 (2000).  
<sup>28</sup> G. Krilov, E. Sim, and B. J. Berne, *J. Chem. Phys.* **114**, 1075 (2001).  
<sup>29</sup> E. Sim, G. Krilov, and B. J. Berne, *J. Phys. Chem.* **105**, 2824 (2001).  
<sup>30</sup> E. Rabani, D. R. Reichman, G. Krilov, and B. J. Berne, *Proc. Natl. Acad. Sci. USA* **99**, 1129 (2002).  
<sup>31</sup> A. A. Golosov, D. R. Reichman, and E. Rabani, *J. Chem. Phys.* **118**, 457 (2003).  
<sup>32</sup> E. Rabani, G. Krilov, D. R. Reichman, and B. J. Berne, *J. Chem. Phys.* **123**, 184506 (2005).  
<sup>33</sup> S. Habershon, B. J. Braams, and D. E. Manolopoulos, *J. Chem. Phys.* **127**, 174108 (2007).  
<sup>34</sup> J. Liu and W. H. Miller, *J. Chem. Phys.* **129**, 124111 (2008).  
<sup>35</sup> F. Paesani and G. A. Voth, *J. Chem. Phys.* **129**, 194113 (2008).  
<sup>36</sup> E. Gallicchio, S. A. Egorov, and B. J. Berne, *J. Chem. Phys.* **109**, 7745 (1998).  
<sup>37</sup> E. Rabani and D. R. Reichman, *J. Chem. Phys.* **120**, 1458 (2004).  
<sup>38</sup> A. W. Sandvik, *Phys. Rev. B* **57**, 10287 (1998).  
<sup>39</sup> F. F. Assaad, *Phys. Rev. B* **78**, 155124 (2008).  
<sup>40</sup> O. F. Syljuåsen, *Phys. Rev. B* **78**, 174429 (2008).  
<sup>41</sup> S. R. White, in D. P. Landau, K. K. Mon, and H.-B. Schuttler, editors, *Computer Simulation Studies in Condensed*

- Matter Physics III*, page 287 (Springer-Verlag, Berlin, 1991).
- <sup>42</sup> K. Mosegaard and A. Tarntola, *J. Geophys. Res.-Sol.* **100**, 12431 (1995).
- <sup>43</sup> A. J. Drummond, G. K. Nicholls, A. G. Rodrigo, and W. Solomon, *Genetics* **161**, 1307 (2002).
- <sup>44</sup> K. S. D. Beach, Identifying the maximum entropy method as a special limit of stochastic analytic continuation, arXiv:cond-mat/0403055.
- <sup>45</sup> J. Liu and W. H. Miller, *J. Chem. Phys.* **128**, 144511 (2008).
- <sup>46</sup> B. J. Berne, *J. Stat. Phys.* **43**, 911 (1986).
- <sup>47</sup> B. J. Berne and D. Thirumalai, *Ann. Rev. Phys. Chem.* **37**, 401 (1986).
- <sup>48</sup> J. Skilling, editor, *Maximum Entropy and Bayesian Methods* (Kluwer, Cambridge, England, 1989).
- <sup>49</sup> F. J. Bermejo, F. J. Mompean, M. Garciahernandez, J. L. Martinez, D. Martinmarero, A. Chahid, G. Senger, and M. L. Ristig, *Phys. Rev. B* **47**, 15097 (1993).
- <sup>50</sup> F. J. Bermejo, B. Fak, S. M. Bennington, R. Fernandez-Perea, C. Cabrillo, J. Dawidowski, M. T. Fernandez-Diaz, and P. Verkerk, *Phys. Rev. B* **60**, 15154 (1999).
- <sup>51</sup> E. Rabani and D. R. Reichman, *Phys. Rev. E* **65**, 036111 (2002).
- <sup>52</sup> D. R. Reichman and E. Rabani, *Phys. Rev. Lett.* **87**, 265702 (2001).
- <sup>53</sup> E. Rabani and D. R. Reichman, *J. Chem. Phys.* **116**, 6271 (2002).
- <sup>54</sup> D. R. Reichman and E. Rabani, *J. Chem. Phys.* **116**, 6279 (2002).
- <sup>55</sup> E. Rabani and D. R. Reichman, *Europhys. Lett.* **60**, 656 (2002).
- <sup>56</sup> F. J. Bermejo, K. Kinugawa, C. Cabrillo, S. M. Bennington, B. Fak, M. T. Fernandez-Diaz, P. Verkerk, J. Dawidowski, and R. Fernandez-Perea, *Phys. Rev. Lett.* **84**, 5359 (2000).
- <sup>57</sup> M. Celli, D. Colognesi, and M. Zoppi, *Phys. Rev. E* **66**, 021202 (2002).
- <sup>58</sup> M. Pavese and G. A. Voth, *Chem. Phys. Lett.* **249**, 231 (1996).
- <sup>59</sup> K. Kinugawa, *Chem. Phys. Lett.* **292**, 454 (1998).
- <sup>60</sup> M. Zoppi, M. Neumann, and M. Celli, *Phys. Rev. B* **65**, 092204 (2002).
- <sup>61</sup> J. A. Poulsen, G. Nyman, and P. J. Rossky, *J. Phys. Chem. B* **108**, 19799 (2004).
- <sup>62</sup> T. Hone and G. A. Voth, *J. Chem. Phys.* **121**, 6412 (2004).
- <sup>63</sup> B. J. Ka and G. A. Voth, *J. Phys. Chem. A* **109**, 11609 (2005).
- <sup>64</sup> T. D. Hone, P. J. Rossky, and G. A. Voth, *J. Chem. Phys.* **124**, 154103 (2006).
- <sup>65</sup> M. Zoppi, U. Bafle, E. Guarini, F. Barocchi, R. Magli, and M. Neumann, *Phys. Rev. Lett.* **75**, 1779 (1995).
- <sup>66</sup> D. Scharf, G. Martyna, and M. L. Klein, *J. Low. Temp. Phys.* **19**, 365 (1993).
- <sup>67</sup> I. F. Silvera and V. V. Goldman, *J. Chem. Phys.* **69**, 4209 (1978).
- <sup>68</sup> I. F. Silvera, *Rev. Mod. Phys.* **52**, 393 (1980).
- <sup>69</sup> E. L. Pollock and D. M. Ceperley, *Phys. Rev. B* **30**, 2555 (1984).
- <sup>70</sup> M. Mukherjee, F. J. Bermejo, B. Fak, and S. M. Bennington, *Europhys. Lett.* **40**, 153 (1997).
- <sup>71</sup> N. Lin, D. R. Reichman, P. Werner, P. S. Cornaglia, A. Georges, and A. J. Millis, Scaling near the correlation and doping-driven metal insulator transition in single-site dynamical mean field theory: new results from analytical continuation, unpublished.